Key Engineering Materials
ISSN: 1662-9795, Vol. 1047, pp 151-160

Submitted: 2026-01-18
Revised: 2026-02-23
Accepted: 2026-02-25
Online: 2026-04-13

Development and Characterization of 3D-Printed PETG Specimens Embedding Continuous Carbon Fiber Strain Sensors

Imi Ochana[1,2,a*], François Ducobu[2,b], Thomas Rainchon[1,c] and Anthonin Demarbaix[1,d]

[1]Science and Technology Research Unit, Haute Ecole Provinciale de Hainaut Condorcet, Boulevard Solvay 31, 6000 Charleroi, Belgium

[2]Machine Design and Production Engineering Lab, Research Institute for Science and Material Engineering, University of Mons, Mons, Belgium

[a*]imi.ochana@condorcet.be, [b]Francois.Ducobu@umons.ac.be, [c]thomas.rainchon@condorcet.be, [d]anthonin.demarbaix@condorcet.be

Keywords: additive manufacturing, PETG composite, continuous carbon fiber, electrical resistivity, structural health monitoring.

Abstract. Continuous monitoring of additively manufactured structures is essential for understanding their mechanical behavior and durability. This study investigates the electromechanical behavior of additively manufactured PETG specimens reinforced with continuous carbon fiber, with a particular focus on the influence of reinforcement geometry on strain-sensing performance. Specimens were fabricated using Fused Filament Fabrication and designed with four different reinforcement configurations: a reference single-layer layout, an extended-length reinforced region, a wider reinforced region, and a double-layer reinforcement. A total of twelve specimens were experimentally characterized. Electrical resistivity measurements were conducted under unloaded conditions and during bending induced by a low applied load of approximately 1.6 N. The initial electrical resistivity was found to depend on reinforcement geometry, with average values of approximately 523 Ω for the reference configuration, 888 Ω for the extended-length reinforcement, 1066 Ω for the wider reinforcement, and 285 Ω for the double-layer configuration. Under mechanical loading, the relative resistance variation remained below 0.6% for all specimens, indicating that the induced strain was very small. To further quantify strain sensitivity, the gauge factor was calculated for each configuration. Low average gauge factor values were obtained for the reference ($K \approx 0.1$), extended-length ($K \approx 0.38$), and wider ($K \approx 0.5$) configurations. In contrast, the double-layer reinforcement exhibited a higher average gauge factor of approximately 2.24. These results indicate that reinforcement architecture affects the electromechanical sensitivity under low applied loads and offer insights for the design of multifunctional additively manufactured composite structures.

Introduction

Since the advent of additive manufacturing (AM), three-dimensional printing has transformed the way complex components are produced, offering new geometric freedom, material efficiency, and the possibility to rapidly iterate designs compared with traditional processes [1]. Among the AM techniques, Fused Filament Fabrication (FFF) is especially widespread due to its relative simplicity, cost-effectiveness, and compatibility with a variety of thermoplastics [2]. However, the layer-by-layer nature of FFF can introduce anisotropy, interlayer adhesion issues, and geometric imperfections, which challenge the mechanical robustness and dimensional stability of printed parts [3]. Beyond the mitigation of these process-related limitations, the incorporation of fiber reinforcements and composite architectures within FFF has emerged as a promising pathway to expand the mechanical capabilities of printed components, enable property tailoring, and meet the requirements of high-performance and load-bearing applications [4]. This approach reflects a broader trend toward multifunctional and application-driven material design, positioning reinforced FFF composites as viable candidates for advanced engineering environments.

In this context, embedding continuous carbon fiber reinforcement within FFF-printed thermoplastic matrices emerges as a promising route to produce lightweight, high-strength composite parts, while also exploiting the multifunctional potential of carbon fibers [5]. Unlike short fiber or particulate fillers, continuous carbon fibers can form percolating conductive pathways throughout the part, offering the dual benefit of enhancing mechanical performance and imparting electrical conductivity [6]. Such carbon fiber-reinforced polymers (CFRPs) fabricated via 3D printing combine the mechanical advantages of classical composites with the design flexibility and rapid manufacturing advantages of AM [7].

These considerations have sparked growing interest in integrating sensing capabilities directly into 3D-printed composite structures. The principle relies on the fact that deformation of a conductive reinforcement, like carbon fiber, produces a change in its electrical resistivity, which can be correlated to the applied mechanical strain [8]. Traditional strain gauges rely on this piezoresistive principle, but embedding continuous conductive fibers into the bulk of a printed part enables the realization of self-sensing structures in a seamless and fully integrated manner [9]. Prior research using conductive filaments has demonstrated the feasibility of in situ strain sensing via FFF printing [10].

Liu et al. [11] investigated the use of additively manufactured continuous carbon fiber reinforced polymers (CCFRPs) as self-sensing materials. By tailoring fiber placement and printing strategies, the authors demonstrated that sensing functionality could be selectively integrated into specific regions of printed components. Their results showed that 3D printed CCFRPs exhibit favorable mechanical behavior together with stable electrical responses, and that key printing parameters, such as extrusion temperature and printing speed, significantly affect these properties. The study further confirmed the capability of CCFRP structures to accurately detect strain and temperature variations, highlighting their potential for integrated sensing applications.

Shafighfard et al. [12] investigated additively manufactured continuous carbon fiber reinforced polymer (CCFRP) components integrating fiber Bragg grating sensors. Their work demonstrated that CCFRP-based sensing structures combine advantageous mechanical properties, such as high stiffness and low weight, with effective sensing capabilities. Experimental results showed high sensitivity and accuracy in applications including structural health monitoring and vibration detection, highlighting the strong potential of 3D printed CCFRP composites for advanced sensor development in engineering applications.

Lanzolla et al. [13]investigated the development of a low-cost strain sensor fabricated via material extrusion additive manufacturing using a conductive PLA-based composite filled with carbon black and carbon nanotubes. The study demonstrated that the additively manufactured sensor exhibits a clear and repeatable correlation between mechanical loading and electrical resistance variation. Although temperature effects and hysteresis were shown to influence repeatability, the sensor achieved high linearity and sensitivity in both force and displacement measurements. These results highlight the potential of conductive polymer-based 3D-printed sensors for low-cost, single-step integration into smart and multifunctional structures.

Chaudhry et al. [14] demonstrated the feasibility of manufacturing continuous carbon fiber reinforced thermoplastic composites using Fused Filament Fabrication. By optimizing process parameters such as the number of reinforced layers and interlayer characteristics, and by employing a modified dual-nozzle system to achieve controlled fiber placement, the authors reported significant mechanical enhancements. For polylactic acid (PLA) matrices, tensile strengths of up to 112 MPa and flexural strengths of 164 MPa were achieved, corresponding to nearly a threefold increase compared to unreinforced PLA. These results underscore the capability of FFF-based continuous fiber reinforcement to produce mechanically robust composite components suitable for industrial applications.

Beyond their contribution to mechanical reinforcement, continuous carbon fibers inherently provide electrical conductivity, which can be exploited to introduce additional functional capabilities into additively manufactured composites.

In this context, integrating continuous carbon fiber reinforcement within FFF-printed parts, and exploiting its electrical conductivity to monitor structural behavior in real time, represents a

compelling approach to design smart, multifunctional composites. In this work, we explore how the geometry of the reinforced zone, in terms of its length, width, and number of fiber layers, influences the electrical sensitivity under mechanical load, and we assess the reproducibility of the fabrication and measurement process. This investigation aims to establish a reliable method for self-sensing 3D-printed composites, capable of continuous structural health monitoring and extending the functionality of additive manufacturing beyond purely structural applications.

Materials and Methods

Specimen Design and Fabrication

Four types of PETG specimens reinforced with continuous carbon fiber were fabricated using FFF on an Anisoprint Composer A4 3D printer to investigate the influence of reinforcement geometry on strain sensing performance. All specimens had identical overall measurements of 190 mm × 40 mm × 2 mm, as illustrated in Fig. 1.

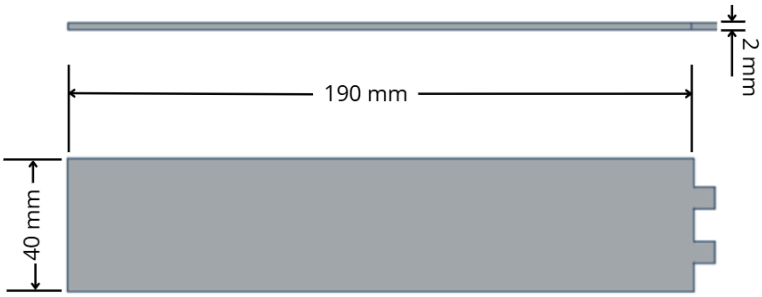

Fig. 1. Measurements of specimens.

The four reinforcement layouts are shown in Fig. 2. For all configurations, each continuous carbon fiber layer had a thickness of 0.4 mm. A reference specimen (1) containing a single continuous carbon fiber reinforcement layer was first produced. Three modified reinforcement configurations were then designed to evaluate the effect of geometric variations: (2) a longer reinforced area with increased length, (3) a wider reinforced area with increased width, and (4) a double-layer reinforced area consisting of two stacked continuous carbon fiber layers. For each configuration, three identical specimens were manufactured to assess fabrication repeatability and measurement reproducibility.

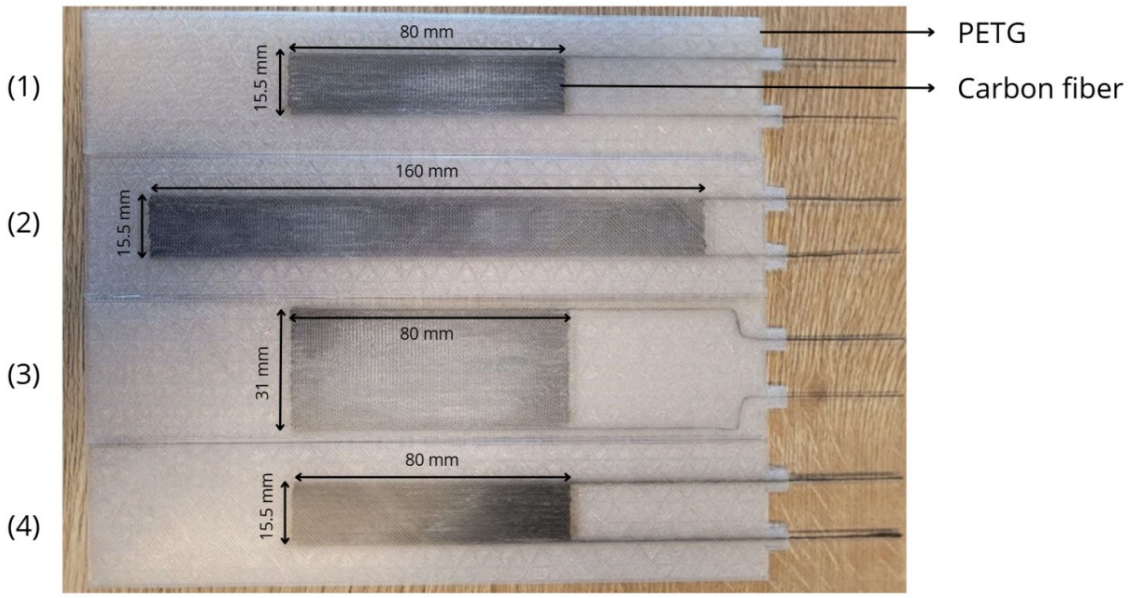

Fig. 2. Four types of PETG specimens reinforced with continuous carbon fiber.

The printing process was controlled to ensure accurate placement and continuity of the carbon fiber within the reinforced regions. Particular attention was paid to maintaining consistent fiber alignment with the PETG matrix across all specimens. This controlled fabrication approach minimized geometric and material variability, allowing the influence of reinforcement geometry on strain sensing behavior to be investigated reliably.

Electrical Measurement

The electrical resistance of the embedded continuous carbon fiber was measured using a Keithley DMM6500 digital multimeter, both in the unloaded state and under applied mechanical loading. Because the carbon fiber reinforcement consists of a single continuous filament embedded within the PETG matrix, it behaves electrically as a one-dimensional conductive path. Consequently, the electrical measurement corresponds to the longitudinal resistance along the fiber axis, between its two exposed ends.

Electrical connections were established using clip cables attached directly to the exposed fiber extremities, ensuring that the measured resistance corresponded to the continuous carbon fiber, as shown in Fig. 3.

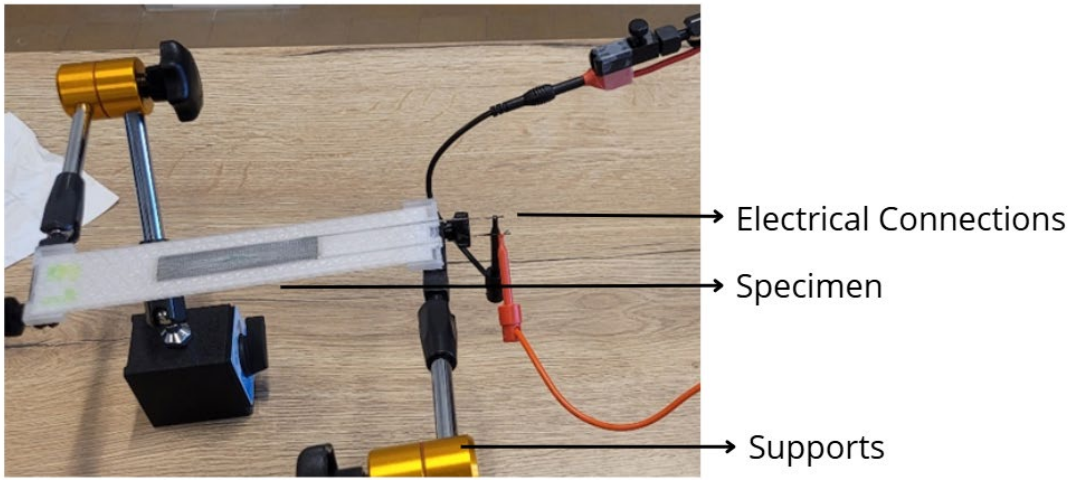

Fig. 3. Electrical connection to the continuous carbon fiber.

For each measurement condition, an initial resistivity measurement was first performed with the specimen in its original orientation. The specimen was then rotated by 180° and the measurement was repeated. This rotation inverted the bending configuration, thereby switching the fiber from the tensile side to the compressive side of the specimen during bending. This procedure allowed evaluation of whether tensile or compressive strain influenced the electrical response of the continuous carbon fiber.

Mechanical Testing Protocol

Mechanical testing was conducted using a simple bending configuration to evaluate the electromechanical response of the specimens under a controlled load case. Each specimen was first placed on two supports, forming a simply supported beam configuration, and electrically connected to the measurement system using a two-wire resistance measurement setup at the specimen connectors.

An initial electrical resistance measurement was recorded in the unloaded state to establish a reference. A calibrated mass of 170 g was then placed at the midpoint of the specimen, as shown in Fig. 4, to induce bending deformation. This mass corresponds to an applied force of approximately 1.6 N and defines the loading condition used throughout the study. Once the load was applied, a second electrical resistance measurement was taken under deformation. This mass was selected to ensure a repeatable and non-perturbing loading condition compatible with the experimental setup (stable placement, no fixture slippage, no contact degradation) while keeping the specimens well

within the linear elastic regime for screening the electromechanical response. The load was kept constant across all tests to enable fair comparison between reinforcement configurations.

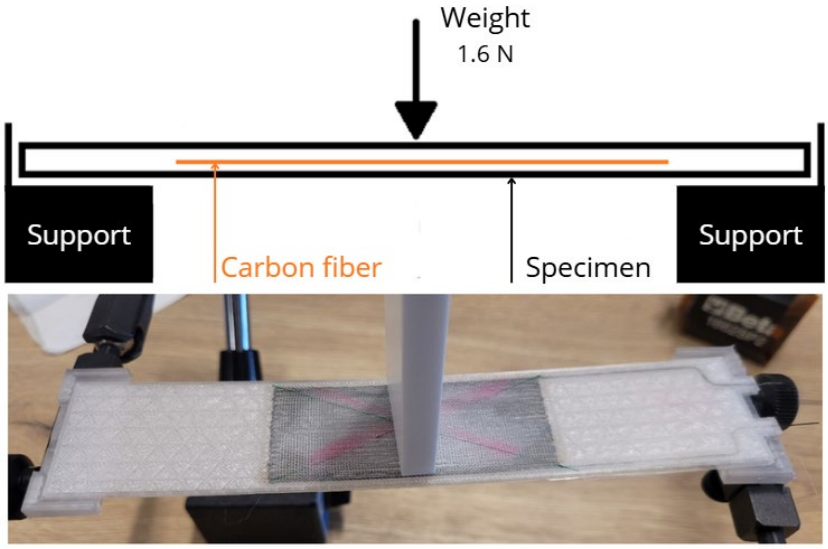

Fig. 4. Mechanical testing set.

This loading–unloading sequence was repeated to ensure measurement repeatability in the initial orientation. The specimen was then disconnected, rotated by 180°, and tested again using the same procedure. Because the specimens were designed to be geometrically symmetric, this additional step was performed to verify that orientation and the inversion of tensile and compressive regions during bending did not introduce measurable differences in the electrical response.

Results and Discussion

A total of twelve specimens were analyzed, with three specimens per configuration. Graph on Fig. 5 shows the initial electrical resistivity values R_0 measured for the four specimen configurations under top-face bending, bottom-face bending and their averaged value. In this study, the terms “top” and “bottom” are defined with respect to the FFF build direction: the bottom face corresponds to the surface formed by the first printed layer in contact with the build platform, while the top face corresponds to the surface formed by the last printed layer. Accordingly, “top-face bending” denotes the configuration where the last-layer surface is oriented on the loaded side, and “bottom-face bending” denotes the configuration where the first-layer surface is oriented on the loaded side.

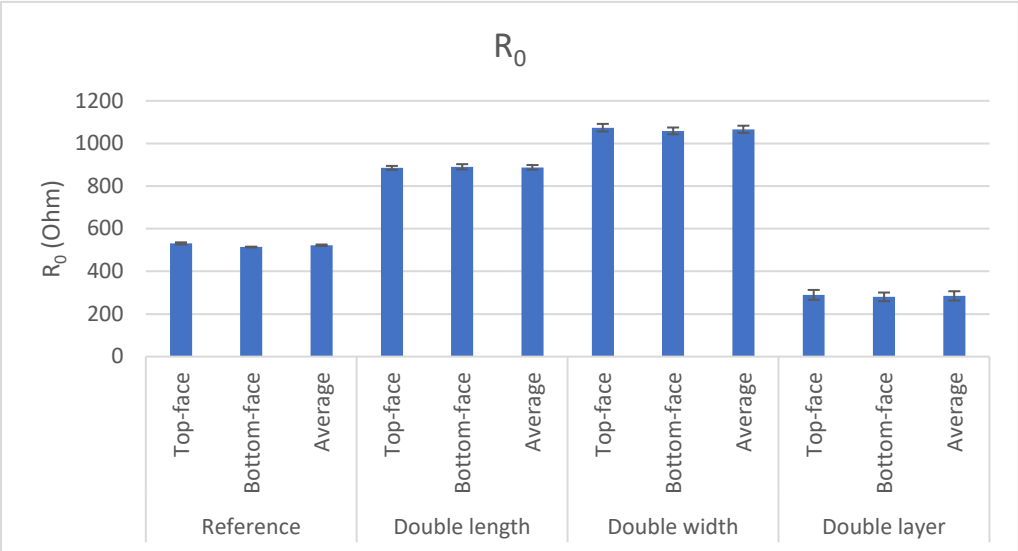

Fig. 5. initial electrical resistivity values R_0.

For the reference specimens, the measured resistivity values range approximately between 514 Ω and 531 Ω, with an average value close to 522 Ω. The difference between the top and bottom bending orientations remains below 5%, indicating a very stable initial electrical behavior and limited sensitivity to specimen orientation for this configuration.

The extended-length reinforcement configuration (Double length) exhibits significantly higher resistivity values, ranging from approximately 885 Ω to 890 Ω, with an average close to 887 Ω. Compared to the reference specimens, this corresponds to an increase in resistivity of approximately 60%, which is consistent with the increased effective fiber length contributing directly to higher electrical resistance.

An even higher resistivity is observed for the wider reinforcement configuration (Double width). In this case, R_0 values are clustered between approximately 1058 Ω and 1073 Ω, yielding an average value around 1066 Ω. This represents an increase of about 50% relative to the reference specimens and approximately 20% compared to the extended-length configuration. A likely explanation for this trend is that increasing the reinforcement width forces the continuous carbon fiber to follow a less direct path, introducing additional zigzag patterns and local deviations. These detours effectively lengthen the electrical conduction path and increase the number of fiber turns, which in turn raises the overall resistance despite the larger nominal width. This finding emphasizes the critical role of fiber trajectory in determining the electrical performance of composite reinforcements.

In contrast, the double-layer reinforcement configuration (Double layer) shows the lowest resistivity values among the modified specimens, with measurements ranging from approximately 280 Ω to 290 Ω and an average value close to 285 Ω. This corresponds to a reduction in resistivity of roughly 45% compared to the reference specimens. This decrease is consistent with the presence of two stacked continuous carbon fiber layers, which effectively act as parallel conductive paths and reduce the overall electrical resistance.

Across all configurations, the difference between top and bottom faces bending orientations remains limited, generally below 5 - 7%. This low dispersion confirms good repeatability of the measurement protocol and indicates that the initial electrical resistivity R_0 is weakly influenced by the bending direction prior to loading. Consequently, the averaged R_0 values provide a reliable baseline for subsequent analysis of strain-induced resistivity variations.

The initial electrical resistivity (R_0) and the resistivity measured under mechanical loading ($R_0 + \Delta R$) are compared in Fig. 6 for the four specimen configurations. The applied load corresponds to the calibrated mass of 170 g positioned at the specimen midpoint, inducing bending deformation. For each configuration, measurements were performed under top-surface bending, bottom-surface bending, and their averaged value. Notably, once the load was removed, the electrical resistance returned to its initial value within the measurement uncertainty, confirming that the specimens remained in the linear elastic regime.

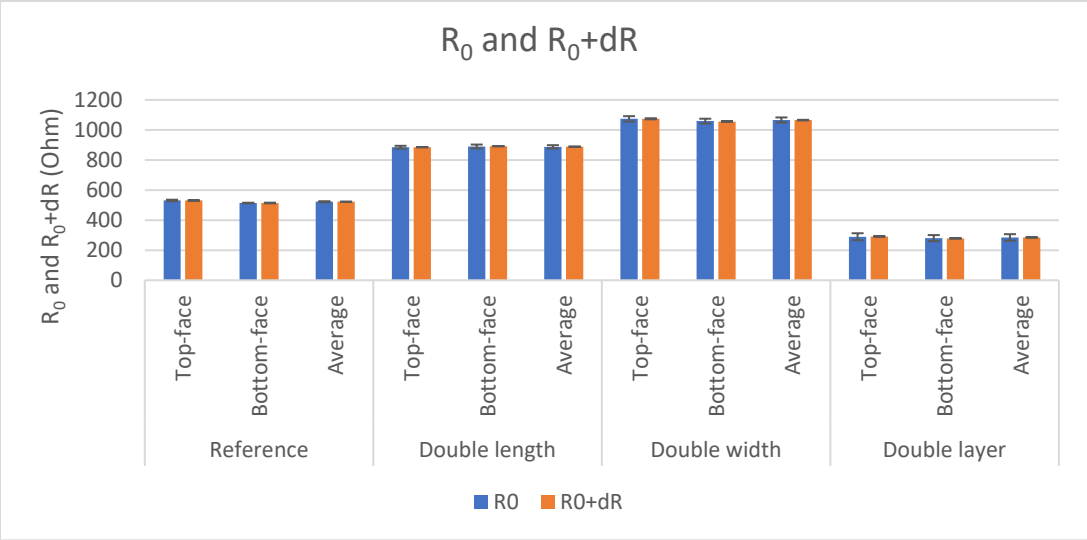

Fig. 6. Initial electrical resistivity (R_0) and resistivity measured under mechanical loading.

For all configurations, the application of the load resulted in negligible changes in electrical resistivity. The averaged relative variation $\Delta R/R_0$ remained below 0.6% for all specimens, which is comparable to the measurement uncertainty of the experimental setup. For the reference specimens, the average resistivity changed from 522.53 Ω to 522.38 Ω, corresponding to a variation of −0.03%. Similarly small variations were observed for the extended-length (+0.10%), wider (−0.09%), and double-layer (+0.06%) reinforcement configurations.

These results indicate that, under the applied load level, the induced bending deformation is insufficient to generate a measurable electromechanical response in the embedded continuous carbon fiber. This suggests that the specimens remain within a very low strain regime, below the sensitivity threshold of the embedded continuous carbon fiber, in which variations in electrical resistance are not yet detectable. Identifying this threshold strain level constitutes an important perspective of the present work and will require experiments conducted under higher and progressively applied bending loads in order to induce larger deformation and activate the electromechanical response of the reinforcement.

Importantly, this behavior also demonstrates the electrical stability and repeatability of the embedded fiber under small mechanical perturbations. The absence of significant resistance variation confirms that the measurement protocol is reliable and that no spurious effects, such as contact instability or electrical noise, dominate the recorded signal.

To further quantify the strain-sensing capability of the embedded continuous carbon fiber, the gauge factor was calculated for all specimens. The gauge factor is defined as the relative change in electrical resistance normalized by the applied mechanical strain and is expressed in Eq. 1.

$$K = \frac{\Delta R/R_0}{\varepsilon} \tag{1}$$

where $R_0$is the initial electrical resistance, $\Delta R = R - R_0$ is the change in resistance under load, and ε is the mechanical strain induced by bending.

The strain used to compute the gauge factor was estimated analytically using composite beam theory. For a simply supported beam subjected to a concentrated load applied at mid-span, the axial strain at the location of the continuous carbon fiber, situated at a distance y from the neutral axis of the composite cross-section, is given in Eq. 2.

$$\varepsilon(\mathrm{y}) = \frac{M_{max} * \mathrm{y}}{(EI)_{eq}} \tag{2}$$

where $(EI)_{eq}$ is the equivalent flexural rigidity of the composite cross-section, computed using the transformed section method with PETG selected as the reference material.

Under the same loading configuration, simply supported beam with a concentrated load applied at mid-span, the maximum bending moment occurs at the center of the span and is given by Eq. 3.

$$M_{max} = \frac{PL}{4} \tag{3}$$

where P is the applied load and L is the span length between the supports.

Fig. 7 presents the calculated gauge factor values for the four specimen configurations under top-face bending, bottom-face bending, and their averaged values. Despite the very small absolute changes in electrical resistance observed under the applied load, the gauge factor analysis reveals clear differences in strain sensitivity between the reinforcement geometries.

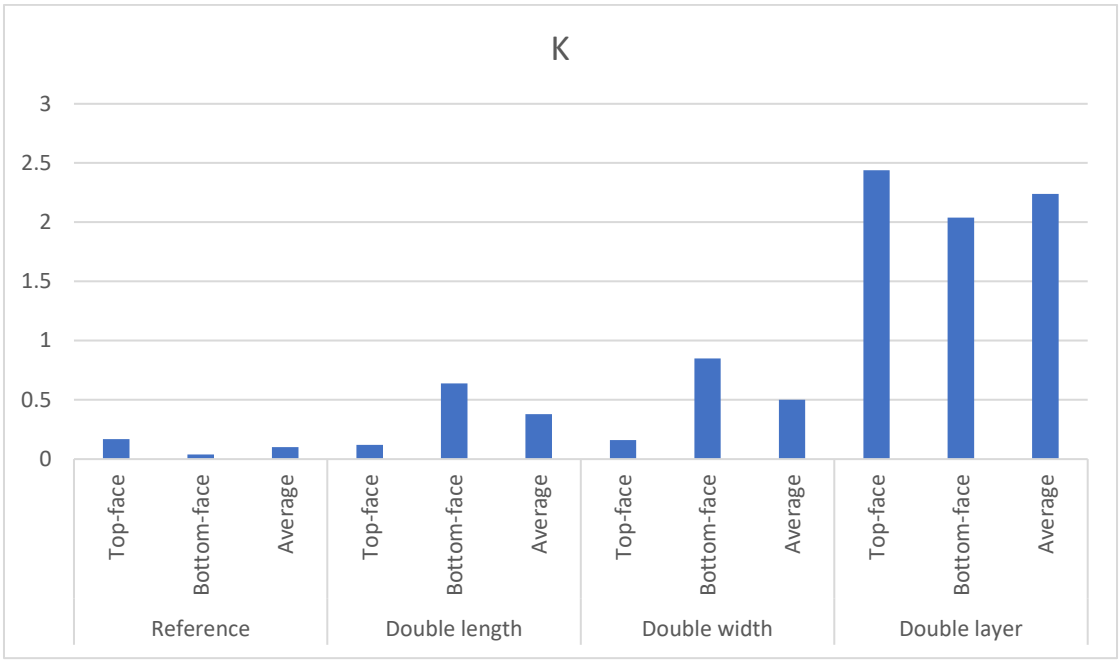

Fig. 7. Gauge factor analysis.

For the reference specimens, very low gauge factor values were obtained, with an average K close to 0.10, associated with a very limited relative resistance variation ($\Delta R/R_0 \approx 0.02\%$). This indicates that, under the applied bending deformation, the embedded carbon fiber exhibits a weak electromechanical coupling and is only marginally affected by the induced strain. The electrical response therefore remains close to the measurement uncertainty, suggesting that the fiber barely perceives the imposed deformation in this configuration.

A slight improvement in strain sensitivity is observed for the extended-length reinforcement configuration, which exhibits an average gauge factor of approximately 0.38 and a relative resistance variation of about 0.10%. The increased specimen length likely promotes a more homogeneous strain distribution along the carbon fiber, resulting in a marginally enhanced transmission of deformation.

The wider reinforcement configuration shows a moderate increase in sensitivity, with an average gauge factor of around 0.50 and a relative resistance variation of approximately 0.12%. Increasing the specimen width alters the stress state within the specimen and appears to improve strain transfer from the polymer matrix to the embedded fiber compared to the reference configuration.

In contrast, the double-layer reinforcement configuration exhibits a markedly enhanced electromechanical response, with an average gauge factor of 2.24 and individual values reaching up to 2.44, together with a significantly higher relative resistance variation ($\Delta R/R_0 \approx 0.57\%$). This corresponds to an increase of more than one order of magnitude in gauge factor compared to the reference specimens. The presence of two stacked carbon fiber layers likely intensifies strain localization and interfacial interactions, leading to a stronger resistance change under bending. Although the absolute resistance variations remain small, these results clearly demonstrate that the reinforcement architecture governs the strain sensitivity. In particular, an appropriate design of the carbon fiber layout can improve sensing performance, even under low applied deformation levels.

Conclusion

This study investigated the electromechanical behavior of PETG specimens reinforced with continuous carbon fiber manufactured by Fused Filament Fabrication using an Anisoprint Composer A4 printer. Four reinforcement geometries were analyzed, including a reference configuration, extended-length and wider reinforced regions, and a double-layer reinforcement, with a total of twelve specimens experimentally characterized.

Electrical resistivity measurements revealed that the initial resistance depends on the reinforcement geometry. Increasing the effective fiber length or width resulted in higher resistivity

values, while the double-layer configuration reduced the overall resistance due to the presence of parallel conductive paths. These trends were consistent across all specimens and confirmed the repeatability of the fabrication and measurement procedures.

Under a low bending load corresponding to a 170 g mass (~1.6 N), only negligible changes in electrical resistivity were observed for all configurations. The relative resistance variations remained below 0.6%, indicating that the applied load induced very small strain levels and that the electrical response of the embedded carbon fiber remained stable in this deformation regime. This behavior also confirms the reliability of the experimental setup and the absence of measurement artifacts related to contact or specimen orientation.

To further assess strain sensitivity, the gauge factor was calculated for all specimens. While low gauge factor values were obtained for the reference, extended-length, and wider reinforcement configurations, the double-layer reinforcement exhibited a higher gauge factor, with an average value of 2.24. This result demonstrates that reinforcement architecture plays a key role in governing electromechanical sensitivity, even under low applied loads, and highlights the potential of stacked continuous carbon fiber layouts for strain-sensing applications.

Overall, the results indicate that although low mechanical loading is insufficient to generate measurable resistance variations in single-layer configurations, appropriate reinforcement design can enhance strain sensitivity. These findings provide valuable insight into the design of multifunctional additively manufactured composite structures. Future research should pursue two complementary directions: first, the application of higher mechanical loads to promote larger strain levels and more effectively activate the strain-sensing behavior of continuous carbon fiber reinforcements; and second, the investigation of alternative mechanical loading modes, such as flexural testing, to better characterize and understand the electromechanical response and sensing potential of the reinforced architectures.

Acknowledgment

The authors would like to thank Région Wallonne for supporting this research as part of the SKYWIN ICOM2C3D research project under grant 8820.

References

[1] M. Pérez, D. Carou, E. M. Rubio, and R. Teti, “Current advances in additive manufacturing,” in *Procedia CIRP*, Elsevier B.V., 2020, pp. 439–444. doi: 10.1016/j.procir.2020.05.076.

[2] I. Ochana, F. Ducobu, L. Spitaels, M. K. Homrani, and A. Demarbaix, “Comparative accuracy analysis of continuous fiber composite printers: Coextrusion vs. dual-nozzle technology,” in *Materials Research Proceedings*, Association of American Publishers, 2024, pp. 127–136. doi: 10.21741/9781644903131-14.

[3] H. Bikas, P. Stavropoulos, and G. Chryssolouris, “Additive manufacturing methods and modeling approaches: A critical review,” *International Journal of Advanced Manufacturing Technology*, vol. 83, no. 1–4, pp. 389–405, Mar. 2016, doi: 10.1007/s00170-015-7576-2.

[4] J. Justo, L. Távara, L. García-Guzmán, and F. París, “Characterization of 3D printed long fibre reinforced composites,” *Compos Struct*, vol. 185, pp. 537–548, Feb. 2018, doi: 10.1016/j.compstruct.2017.11.052.

[5] B. Chang, X. Li, P. Parandoush, S. Ruan, C. Shen, and D. Lin, “Additive manufacturing of continuous carbon fiber reinforced poly-ether-ether-ketone with ultrahigh mechanical properties,” *Polym Test*, vol. 88, Aug. 2020, doi: 10.1016/j.polymertesting.2020.106563.

[6] D. G. Bekas, Y. Hou, Y. Liu, and A. Panesar, “3D printing to enable multifunctionality in polymer-based composites: A review,” Dec. 15, 2019, *Elsevier Ltd*. doi: 10.1016/j.compositesb.2019.107540.

[7] Z. Wang, C. Luan, G. Liao, X. Yao, and J. Fu, “Mechanical and self-monitoring behaviors of 3D printing smart continuous carbon fiber-thermoplastic lattice truss sandwich structure,” *Compos B Eng*, vol. 176, Nov. 2019, doi: 10.1016/j.compositesb.2019.107215.

[8] A. Demarbaix, I. Ochana, J. Levrie, I. Coutinho, S. S. Cunha, and M. Moonens, “Additively Manufactured Multifunctional Composite Parts with the Help of Coextrusion Continuous Carbon Fiber: Study of Feasibility to Print Self-Sensing without Doped Raw Material,” *Journal of Composites Science*, vol. 7, no. 9, Sep. 2023, doi: 10.3390/jcs7090355.

[9] I. Ochana, F. Ducobu, M. K. Homrani, and A. Demarbaix, “Design of experiment on smart materials: tensile test on 3D printed composites reinforced with continuous carbon fiber and resistivity detection,” in *Materials Research Proceedings*, Association of American Publishers, 2025, pp. 49–58. doi: 10.21741/9781644903599-6.

[10] I. U. Musa, R. A. Gomes, M. Sonego, and G. F. Gomes, “Advances in embedded sensor technologies for structural health monitoring of composite structures: a comprehensive review,” 2025, *Taylor and Francis Ltd.* doi: 10.1080/10589759.2025.2581826.

[11] G. Liu, Y. Xiong, and L. Zhou, “Additive manufacturing of continuous fiber reinforced polymer composites: Design opportunities and novel applications,” Oct. 01, 2021, *Elsevier Ltd*. doi: 10.1016/j.coco.2021.100907.

[12] T. Shafighfard and M. Mieloszyk, “Experimental and numerical study of the additively manufactured carbon fibre reinforced polymers including fibre Bragg grating sensors,” *Compos Struct*, vol. 299, Nov. 2022, doi: 10.1016/j.compstruct.2022.116027.

[13] A. M. L. Lanzolla, F. Attivissimo, G. Percoco, M. A. Ragolia, G. Stano, and A. Di Nisio, “Additive Manufacturing for Sensors: Piezoresistive Strain Gauge with Temperature Compensation,” *Applied Sciences (Switzerland)*, vol. 12, no. 17, Sep. 2022, doi: 10.3390/app12178607.

[14] F. N. Chaudhry, S. I. Butt, A. Mubashar, A. Bin Naveed, S. H. Imran, and Z. Faping, “Effect of carbon fibre on reinforcement of thermoplastics using FDM and RSM,” *Journal of Thermoplastic Composite Materials*, vol. 35, no. 3, pp. 352–374, Mar. 2022, doi: 10.1177/0892705719886891.